Genes & Diseases xxx (xxxx) xxx

Available online at www.sciencedirect.com

ScienceDirect

journal homepage: http://ees.elsevier.com/gendis/default.asp

FULL LENGTH ARTICLE

Integrated analysis reveals the protective mechanism and therapeutic potential of hyperbaric oxygen against pulmonary fibrosis

Yuan Yuan [a,1], Guoqiang Qiao [a,1], Jiajiao Zhou [a], Yilu Zhou [b,c], Yali Li [a], Xia Li [a,**], Zhenglin Jiang [a,***], Yihua Wang [b,c,*]

[a] *Department of Neurophysiology and Neuropharmacology, Institute of Special Environmental Medicine and Co-innovation Center of Neuroregeneration, Nantong University, Nantong, Jiangsu 226019, PR China*
[b] *Biological Sciences, Faculty of Environmental and Life Sciences, University of Southampton, Southampton, SO17 1BJ, United Kingdom*
[c] *Institute for Life Sciences, University of Southampton, Southampton, SO17 1BJ, United Kingdom*

Received 27 April 2022; received in revised form 1 August 2022; accepted 20 August 2022

KEYWORDS
Epithelial-mesenchymal transition;
Hyperbaricoxygen;
Hypoxia;
Pulmonary fibrosis;
Systematic analysis

Abstract Idiopathic pulmonary fibrosis (IPF) is a dreadful, chronic, and irreversibly progressive disease leading to death with a few effective treatments. Our previous study suggested that repetitive hyperbaric oxygen (HBO) treatment alleviates bleomycin-induced pulmonary fibrosis in mice. Here, we investigated the protective mechanism of HBO treatment against pulmonary fibrosis using an integrated approach. Analyzing publicly available expression data from the mouse model of bleomycin-induced pulmonary fibrosis as well as IPF patients, several potential mechanisms of relevance to IPF pathology were identified, including increased epithelial-to-mesenchymal transition (EMT) and glycolysis. High EMT or glycolysis scores in bronchoalveolar lavage were strong independent predictors of mortality in multivariate analysis. These processes were potentially driven by hypoxia and blocked by HBO treatment. Together, these data support HBO treatment as a viable strategy against pulmonary fibrosis.

* Corresponding author. Biological Sciences, Faculty of Environmental and Life Sciences, University of Southampton, Southampton, SO17 1BJ, United Kingdom.
** Corresponding author.
*** Corresponding author.
E-mail addresses: lixia7979@ntu.edu.cn (X. Li), jiangzl@ntu.edu.cn (Z. Jiang), yihua.wang@soton.ac.uk (Y. Wang).
Peer review under responsibility of Chongqing Medical University.
[1] These authors contributed equally and share the first authorship.

https://doi.org/10.1016/j.gendis.2022.08.012

Please cite this article as: Yuan Y et al., Integrated analysis reveals the protective mechanism and therapeutic potential of hyperbaric oxygen against pulmonary fibrosis, Genes & Diseases, https://doi.org/10.1016/j.gendis.2022.08.012

Introduction

Idiopathic pulmonary fibrosis (IPF) is a chronic, progressive and fatal interstitial lung disease, characterized by excessive deposition of extracellular matrix (ECM) in the lung parenchyma, leading to the destroyed alveolar architecture and disrupted lung functions. It has a poor prognosis and limited treatment options.[1] Recently, pulmonary fibrosis is reported to be a long-term outcome associated with major morbidity after COVID-19 infection,[2–4] therefore, draws increasing attention. Novel and effective approaches to treat pulmonary fibrosis are urgently needed.

Previously we reported that hyperbaric oxygen (HBO) treatment attenuates a single dose of intratracheal administrated bleomycin-induced pulmonary fibrosis in mice,[5] however, the underlying molecular mechanism is to be clarified. HBO treatment is to inhale pure oxygen under a pressure of more than 1 atmosphere absolute (ATA). It significantly increases the dissolved oxygen in plasma and the diffusion distance of oxygen, therefore, is applied in clinics for the treatment of a variety of diseases with underlying hypoxia.[6] Here we sought to investigate the protective mechanism of HBO treatment against pulmonary fibrosis using an integrated approach.

Materials and methods

Integrative analysis

The flow charts of data collection from the bleomycin-induced mouse model (microarray) and IPF patients (RNA-seq) are provided in Figure S1, with a summary of datasets in Table S1—S3. A detailed description of data merging analysis, including uniform manifold approximation and projection (UMAP) analysis, differential expression genes (DEGs) analysis, gene ontology (GO) enrichment, and gene set enrichment analysis (GSEA), is provided in the Supplementary methods.

Animal experiments

Animals used in this study were purchased from the Experimental Animal Center of Nantong University (Institutional License: SYXK (SU)-2012-0030). Mice were maintained in the individually ventilated cages, under a 12-h light/12-h dark cycle, and were allowed to eat and drink *ad libitum* throughout the study. Animal experiments in this study were approved by the Animal Ethics Committee at Nantong University (Approval No: S20200315-005), and all the experiments conformed to the relevant regulatory standards. The bleomycin-induced pulmonary fibrosis mouse model was constructed and treated with HBO as previously reported.[5] The hematoxylin and eosin (H/E) staining was performed to confirm the presence of pulmonary fibrosis. The details of these experiments can be found in the Supplementary methods.

RNA-seq and bioinformatic analysis

RNA isolation and mRNA sequencing of lung tissues were performed following the manufacturer's instructions. Paired-end strategy (2×150) on the Illumina NovaSeq 6000 platform was adopted. The quality control of raw reads, mapping, identification of DEGs, as well as GO term enrichment analysis and GSEA were performed with details provided in the Supplementary methods. The RNA-seq data have been deposited in the Gene Expression Omnibus (GEO) database (accession code GSE200109).

Gene set variation analysis (GSVA) score calculation

To assess the activity of a specific pathway, GSVA package[7] (version 1.40.1) was used to calculate the score. The Hallmark gene sets of epithelial—mesenchymal transition (EMT) and glycolysis were used to calculate EMT and glycolysis scores, respectively. A 15-gene expression signature (*ACOT7*, *ADM*, *ALDOA*, *CDKN3*, *ENO1*, *LDHA*, *MIF*, *MRPS17*, *NDRG1*, *P4HA1*, *PGAM1*, *SLC2A1*, *TPI1*, *TUBB6*, and *VEGFA*), which enables classification of hypoxia-inducible factor (HIF) activity,[8,9] was used to calculate the HIF score.

Hazard ratio and survival analysis

To assess the hazard ratio (HR), EMT score and glycolysis score were used to construct the univariate Cox proportional hazards model through survminer (version 0.4.9) in RStudio. The log-rank tests were used to compare Kaplan—Meier survival curves between each group by the survival package (v3.2-3). EMT score, glycolysis score, and GAP (gender, age, physiological) score, which is provided in GSE70867[10], were used to construct the multivariate Cox proportional hazard model via the survminer (version 0.4.9) in RStudio. The log-rank and Cox $P < 0.05$ were considered statistically significant.

Real-time quantitative PCR (qPCR) analysis

Genes of interest were detected by RT-qPCR using SYBR green as the indicator. The details of the experimental process, as well as primers, are provided in the Supplementary methods.

Western blot analysis

Protein samples from mice lung tissues were lysed with Radio-Immunoprecipitation Assay (RIPA) buffer (Beyotime

Please cite this article as: Yuan Y et al., Integrated analysis reveals the protective mechanism and therapeutic potential of hyperbaric oxygen against pulmonary fibrosis, Genes & Diseases, https://doi.org/10.1016/j.gendis.2022.08.012

Biotechnology, China) containing protease inhibitor (Meilunbio, Liaoning, China). Primary antibodies targeting E-cadherin (Cat#3195, Cell Signaling Technology, USA) and β-actin (Cat#A5316, Sigma-Aldrich, USA) were used. Signals were detected using an Enhanced chemiluminescence detection system with Tanon 5200 Multi imaging system (Shanghai, China), and evaluated by ImageJ 1.42q software (National Institutes of Health).

Lactate measurement

The lactate levels in the lung tissues were detected by the L-lactic acid/lactate (LA) colorimetric assay kit (Cat#E-BC-K044-M, Elabscience Biotechnology, China) following the manufacturer's instructions.

Statistical analysis

Statistical analyses were performed in GraphPad Prism (version 9.0). Data are presented as mean and standard deviation (s.d.). The choice of analytical method depends on whether the data follow a normal distribution and variance homogeneity. The comparison between the two groups was performed using either two-sample *t*-test or Mann—Whitney *U* test. A false discovery rate calculated through the two-stage step-up method of the Benjamini, Krieger and Yekutieli method was adopted in the multiple comparisons. One-way ANOVA or Kruskal—Wallis test was used to compare more than two groups of data. The Dunnett test was used for multiple comparisons. We evaluated the correlations between the EMT score, Glycolysis score and HIF score using Pearson's correlation. Results were considered significant as $P < 0.05$ or false discovery rate (FDR) $Q < 0.05$.

Code availability

Codes were implemented in R and have been deposited in GitHub: https://github.com/claw60/IPF.

Data availability

All data supporting the findings of the current study are listed in the Supplementary materials.

Results

Integrative analysis reveals the activation of EMT and glycolysis in pulmonary fibrosis

A total of 213 murine lung samples were collected from 10 GEO datasets (Fig. S1A), including 90 control lungs and 123 bleomycin-challenged lungs collected at different time points (Table S1, S2). After batch effects removal by cross-platform normalization, 2 clear clusters corresponding to control and bleomycin-challenged lungs, respectively, were visualized using UMAP analysis (Fig. S2). A total of 6914 genes, which were present in all the samples, were included in the following analysis. In addition, 6 GEO datasets of human lung samples were collected, including 167 control lungs from healthy donors and 205 IPF lungs (Fig. S1B and Table S3). Following batch effects removal, samples were classified into control and IPF groups (Fig. S3). DEGs were identified followed by further analysis (Fig. S4 and Tables S4—S11). Details of the protocol were provided in the Supplementary method.

GO enrichment analysis identified several IPF-related pathological terms, including extracellular matrix and collagen (Table S12—S19). GSEA based on the 50 well-characterized hallmark gene sets from the Molecular Signature Database (MSigDB)[11] identified the activation of EMT and glycolysis in bleomycin-challenged mice lungs at different time points, in IPF lungs as well as bronchoalveolar lavage (BAL) samples from IPF patients[10] (Fig. 1A).

The activation of EMT in bleomycin-challenged mice lungs (Fig. S5) was verified by checking the expression levels of several EMT markers, including *Cdh1* (encoding E-cadherin, an epithelial marker), *Vim* (encoding vimentin, a mesenchymal marker), *Mmp2* (encoding matrix metallopeptidase 2), *Acta2* (encoding α-smooth muscle actin, α-SMA, a myofibroblast marker), *Fn1* (encoding fibronectin) and *Col1a1* (encoding type I collagen). We observed a decrease in the level of *Cdh1* and an increase in the levels of *Vim*, *Mmp2*, *Acta2*, *Fn1*, and *Col1a1* in bleomycin-challenged mice lungs at day 7 or day 21 post instillation (Fig. 1B, C). These results confirmed activation of EMT in the development of pulmonary fibrosis induced by bleomycin in mice.

EMT and glycolysis scores in BAL predict mortality in IPF patients

We next investigated whether EMT and glycolysis scores had prognostic values in the BAL cohort. IPF patients were classified into score-high or score-low groups based on an optimal cutoff value automatically determined by the algorithm. We identified that both the EMT score and glycolysis score were able to predict survival in the IPF cohort (Fig. 2A, B; hazard ratio, HR: 23 and $P = 1.41 \times 10^{-8}$ for the EMT score; HR: 19 and $P = 8.71 \times 10^{-6}$ for the glycolysis score). Multivariate analysis suggested that a high EMT score or a high glycolysis score was a strong independent predictor of mortality including in multivariate analysis with the physiological GAP score that uses commonly measured clinical and physiologic variables to predict mortality in IPF[12] (Fig. 2C; HR: 12.4 and $P < 0.001$ for the EMT score; HR: 5.1, $P = 0.036$ for the glycolysis score).

EMT and glycolysis activation during pulmonary fibrosis is potentially driven by hypoxia

Hypoxia is known to activate EMT and glycolysis.[13—16] In consistence with a recent report,[17] the HIF score, an indicator of hypoxia-inducible factor (HIF) activity calculated using a 15 gene signature,[8,9] was significantly increased in IPF lungs (Fig. 3A) as well as BAL samples (Fig. 3B) from IPF patients. In addition, the HIF score was elevated in bleomycin-challenged mice lungs from day 2 to day 21 post instillation (Fig. 3C). The induction of HIF activity in bleomycin-challenged mice lungs (Fig. S5) was further verified

Please cite this article as: Yuan Y et al., Integrated analysis reveals the protective mechanism and therapeutic potential of hyperbaric oxygen against pulmonary fibrosis, Genes & Diseases, https://doi.org/10.1016/j.gendis.2022.08.012

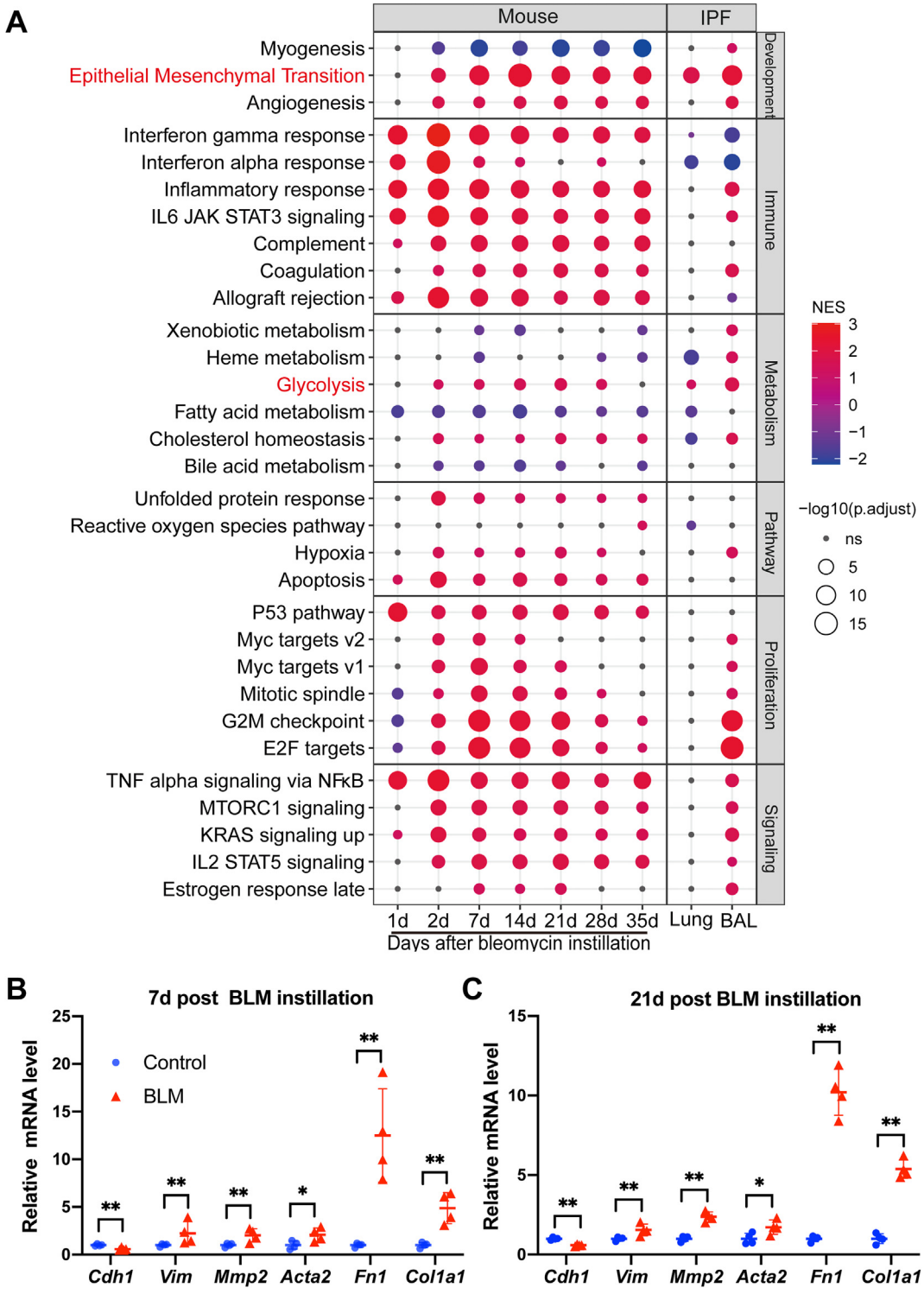

Fig. 1 Integrative analysis reveals the activation of epithelial-to-mesenchymal transition (EMT) and glycolysis in pulmonary fibrosis. **(A)** Scatter plot showing gene set enrichment analysis (GSEA) from 6 categories (development, immune, metabolism, pathway, proliferation, and signaling). The sizes of circles represent the −Log10 of the adjusted *P* values and the colors of circles represent the normalized enrichment score (NES). **(B, C)** Fold change in the mRNA levels of EMT markers in the lungs from saline-treated (Control) or bleomycin-challenged mice (BLM) at day 7 (B) or day 21 (C) post instillation. *Actb* (β-actin) -normalized mRNA levels in the control group were used to set the baseline value at unity. Data are expressed as mean ± s.d.*$Q < 0.05$, **$Q < 0.01$, by two sample Mann−Whitney *U* test, multiple comparisons using false discovery rate (*Q*) with the method of two-stage step-up (Benjamini, Krieger and Yekutieli).

Please cite this article as: Yuan Y et al., Integrated analysis reveals the protective mechanism and therapeutic potential of hyperbaric oxygen against pulmonary fibrosis, Genes & Diseases, https://doi.org/10.1016/j.gendis.2022.08.012

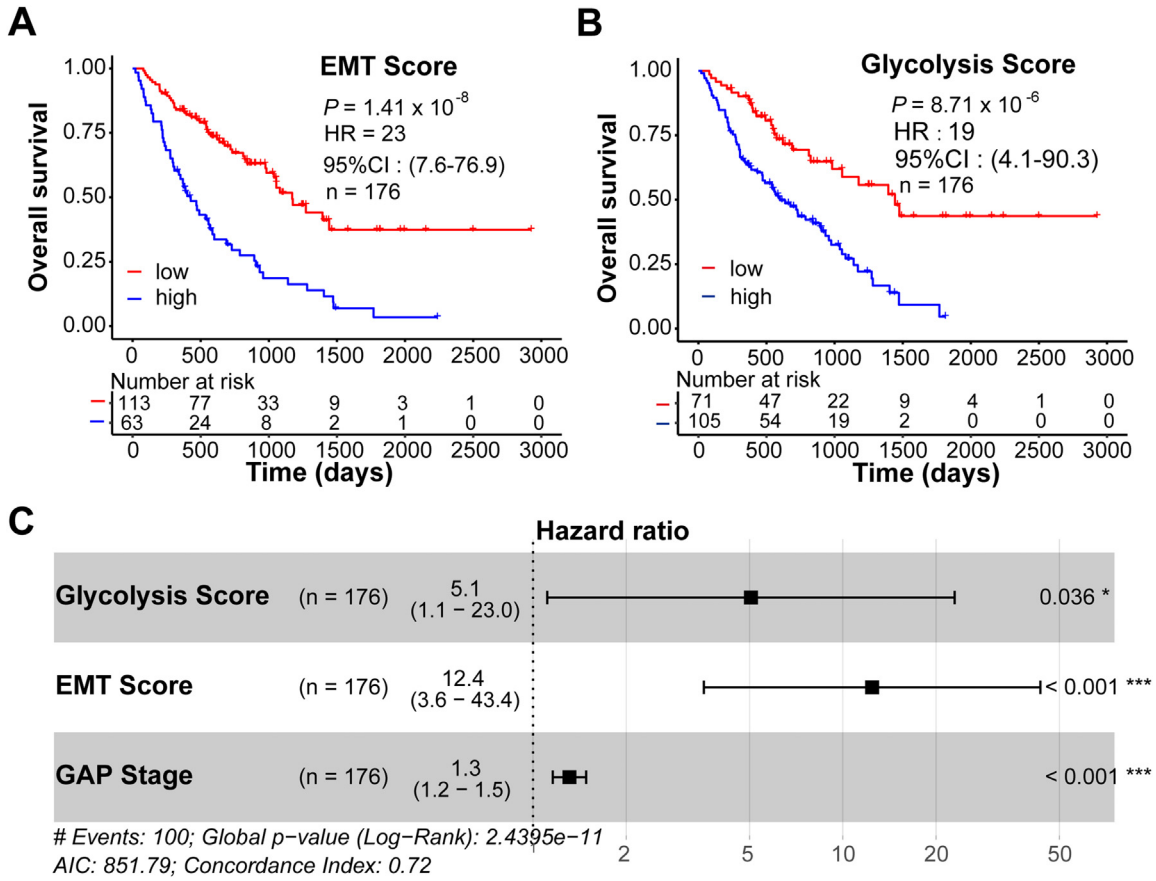

Fig. 2 Epithelial-to-mesenchymal transition (EMT) and glycolysis scores in bronchoalveolar lavage (BAL) predict mortality in IPF patients. **(A, B)** Kaplan–Meier plots show the overall survival in idiopathic pulmonary fibrosis (IPF) patients with low *vs*. high EMT scores (A) or glycolysis scores (B) in BAL. *P* values, hazard ratio (HR), 95% confidence interval (CI), and patient number (*n*) are indicated. **(C)** Multivariate analysis in IPF patients. HR, 95% CI, patient number (*n*) and *P* values are shown.

by checking the expression levels of these 15 genes,[8,9] including *ACOT7*, *ADM*, *ALDOA*, *CDKN3*, *ENO1*, *LDHA*, *MIF*, *MRPS17*, *NDRG1*, *P4HA1*, *PGAM1*, *SLC2A1*, *TPI1*, *TUBB6*, and *VEGFA*, in mice lungs at day 7 and day 21 post bleomycin treatment.

Among the 15 genes, *PGAM1*, *TPI1*, *MIF*, *ALDOA*, *LDHA*, *ENO1*, *VEGFA*, and *P4HA1* are also included in the Hallmark glycolysis gene set, therefore can partially represent the glycolysis status as well. On day 7 post bleomycin treatment, the expression levels of *Adm*, *Aldoa*, *Cdkn3*, *Eno1*, *Ndrg1*, *Pgam1*, *Slc2a1*, *Tpi1*, and *Tubb6* were all elevated (all $Q < 0.05$). There was a trend of increase in the expression level of *Acot7* and *Mif*, although statistical significance wasn't reached ($Q = 0.06$ and $Q = 0.09$, respectively). On day 21 post bleomycin treatment, the expression levels of *Adm*, *Aldoa*, *Cdkn3*, *Eno1*, *Mif*, *Mrps17*, *Slc2a1*, and *Tpi1* were all significantly upregulated (all $Q < 0.01$) (Fig. 3D, E). Together, these results demonstrated that HIF activity is induced in mice lungs upon bleomycin challenge.

We then investigated whether EMT and glycolysis activation occurs during the development of pulmonary fibrosis in the context of hypoxia. The HIF score correlated strongly with an EMT signature in IPF lungs (Fig. 3F; $R = 0.47$, $P = 2.6 \times 10^{-16}$), BAL samples (Fig. 3G; $R = 0.42$, $P = 6.3 \times 10^{-10}$) and bleomycin-challenged mice lungs (Fig. 3H; $R = 0.56$, $P = 2.3 \times 10^{-16}$). These correlations were also observed between the HIF score and glycolysis score (Fig. 3I–K).

The protective mechanism of HBO against pulmonary fibrosis

We previously reported that repetitive HBO treatment started from day 7 post bleomycin instillation significantly alleviates lung fibrosis in mice (Fig. 4A, B).[5] To determine the underlying molecular mechanism, we characterized the global transcriptomic changes in bleomycin-challenged mice lungs exposed to HBO by performing RNA-Seq. Genes with a *P* value less than 0.05 and fold change above 1.5 were considered as DEGs. In total, 1221 DEGs were identified, including 651 upregulated and 570 downregulated genes (Fig. 4C and Table S20). GO enrichment analysis identified "extracellular matrix" as the top enriched term in down-regulated genes for the cellular component classification, consistent with our previous findings[18] (Fig. 4D and Table S21). GSEA identified several pathways inhibited upon HBO treatment in bleomycin-challenged mice lungs, including the above identified EMT, glycolysis, and hypoxia

Please cite this article as: Yuan Y et al., Integrated analysis reveals the protective mechanism and therapeutic potential of hyperbaric oxygen against pulmonary fibrosis, Genes & Diseases, https://doi.org/10.1016/j.gendis.2022.08.012

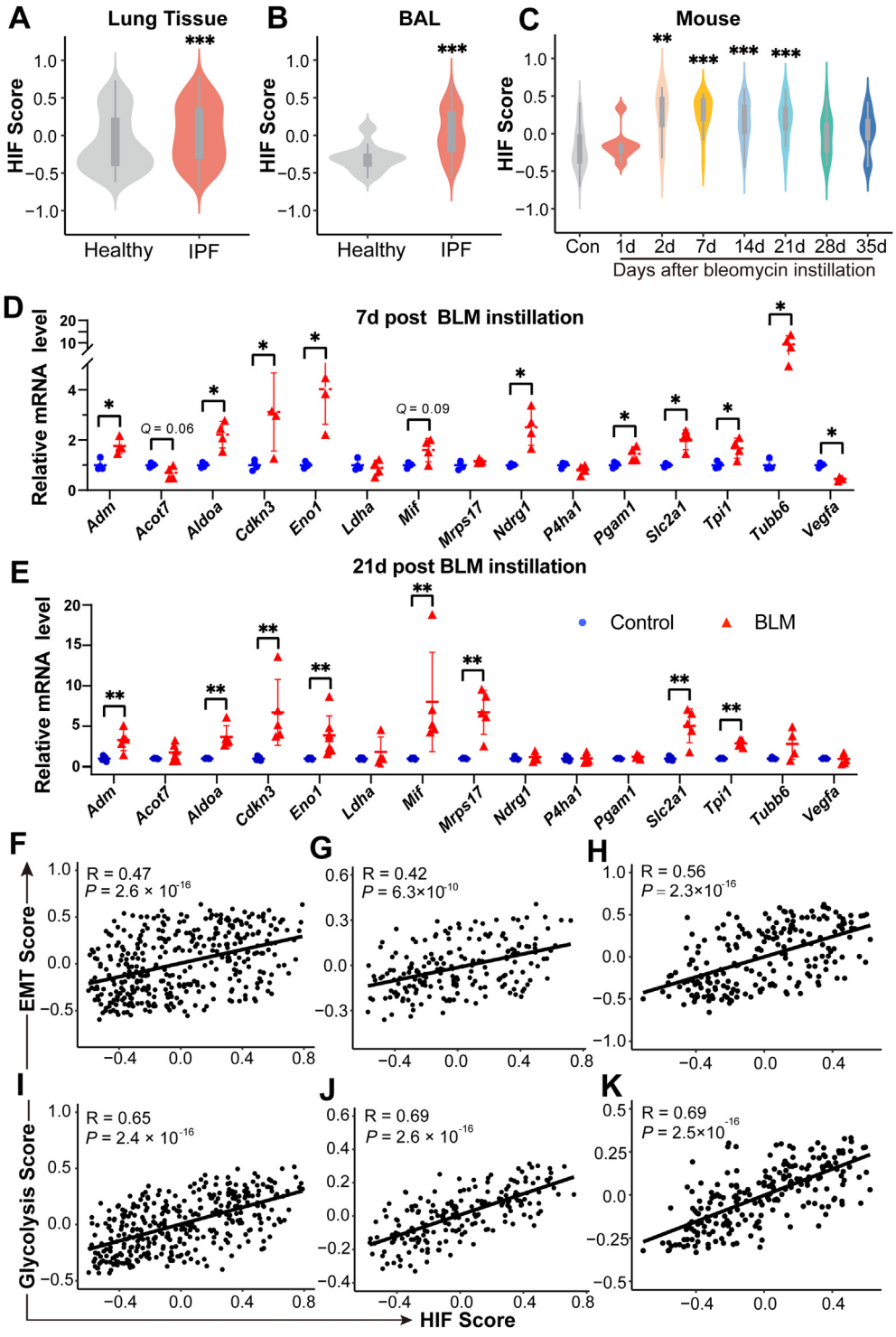

Fig. 3 Epithelial-to-mesenchymal transition (EMT) and glycolysis activation during pulmonary fibrosis is potentially driven by hypoxia. **(A, B)** Violin plots showing hypoxia-inducible factor (HIF) scores in the lungs (A) and bronchoalveolar lavage (BAL) samples (B) from healthy control *vs*. IPF patients. ***$P < 0.001$, by two sample Mann—Whitney *U* test. **(C)** Violin plot showing HIF scores in the lungs from control or bleomycin-treated mice at multiple time points post instillation. **$P < 0.01$, ***$P < 0.001$, by Dunnett's multiple comparisons test. **(D, E)** Fold change in the mRNA levels of multiple HIF target genes in the lungs from saline-treated (Control) or bleomycin-challenged mice (BLM) at day 7 (D) or day 21 (E) post instillation. *Actb* (β-actin)-normalized mRNA levels in the control group were used to set the baseline value at unity. Data are mean ± s.d. *$Q < 0.05$, **$Q < 0.01$, by two sample Mann—Whitney *U* test, multiple comparisons using false discovery rate (*Q*) with the method of two-stage step-up (Benjamini, Krieger and Yekutieli). **(F—H)** Scatter plots showing the correlation between the HIF score and EMT score in IPF lungs (F), BAL samples, (G) and lungs from bleomycin-challenged mice (H). **(I—K)** Scatter plots showing the correlation between HIF score and glycolysis score in IPF lungs (I), BAL samples (J), and lungs from bleomycin-challenged mice (K). Pearson *R*-values and *P* values are indicated.

Please cite this article as: Yuan Y et al., Integrated analysis reveals the protective mechanism and therapeutic potential of hyperbaric oxygen against pulmonary fibrosis, Genes & Diseases, https://doi.org/10.1016/j.gendis.2022.08.012

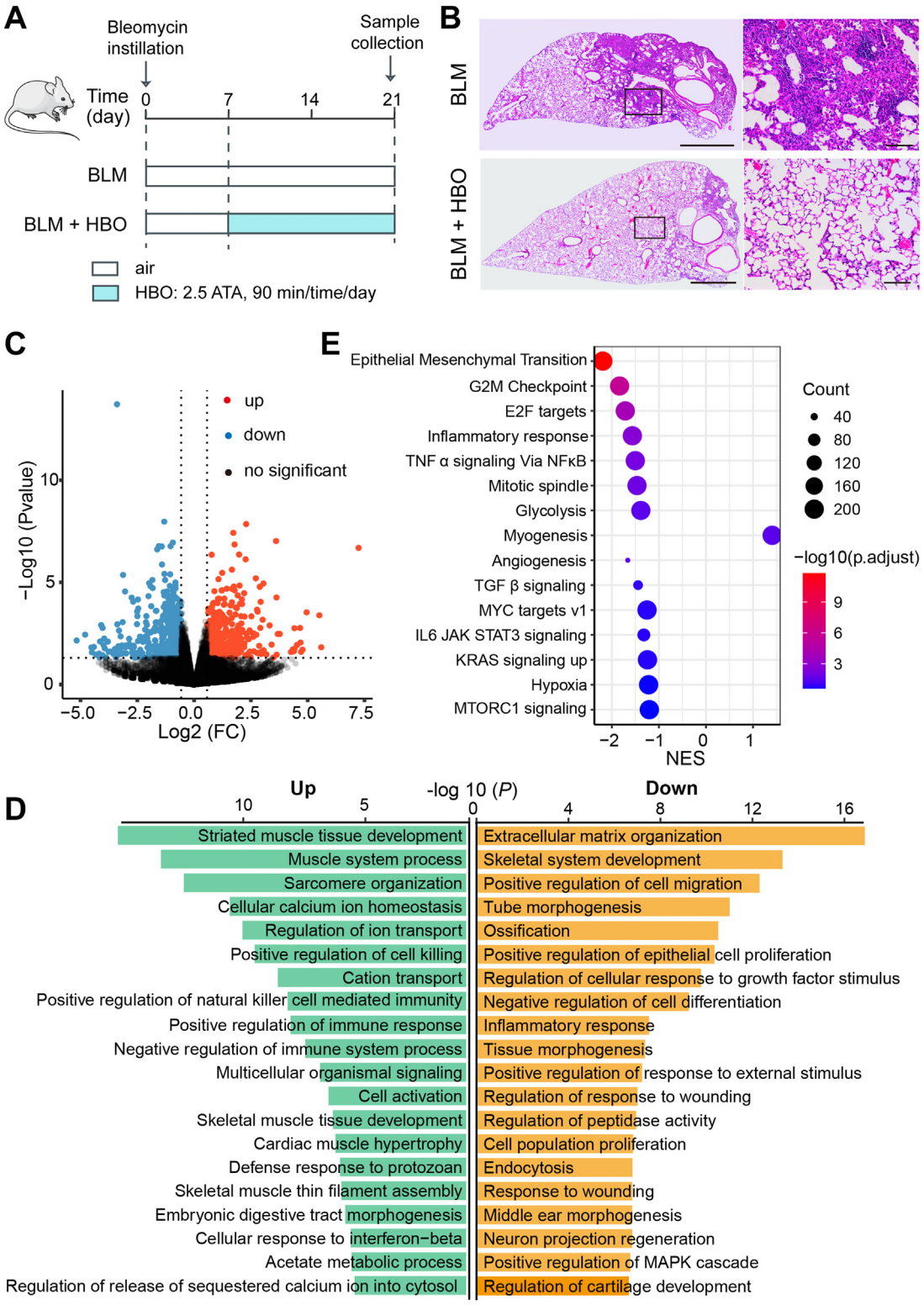

Fig. 4 The protective mechanism of hyperbaric oxygen (HBO) against pulmonary fibrosis. **(A)** Schematic diagram of the experimental procedure (details in the Supplementary methods). **(B)** Lung tissues from bleomycin-challenged mice (BLM) or bleomycin-challenged mice treated with repetitive HBO exposure (BLM + HBO) were stained with H/E. The left panel shows the whole section of the left lung lobe (scale bar: 1 mm) with higher magnification images of the box area in the corresponding right panel (scale bar: 100 μm). **(C, D)** Global transcriptomic changes are identified in bleomycin-challenged mice lungs exposed to HBO by performing RNA-Seq. **(C)** Volcano plot showing differential expression genes (DEGs) ($P < 0.05$ and fold change >1.5) analyzed by DEseq2. Up- and down-regulated genes are highlighted in red and blue, respectively. **(D)** Bar chart summarizing GO enrichment results analyzed by Metascape. Up- and down-regulated terms, as well as −log10 (P), are indicated. **(E)** Bubble chart showing the gene set enrichment analysis (GSEA) results. The sizes of circles represent the count of genes detected in the pathway and the colors of circles represent the −Log10 of the adjusted *P* values. NES represents the normalized enrichment score.

Please cite this article as: Yuan Y et al., Integrated analysis reveals the protective mechanism and therapeutic potential of hyperbaric oxygen against pulmonary fibrosis, Genes & Diseases, https://doi.org/10.1016/j.gendis.2022.08.012

(Fig. 4E). The findings were further confirmed by GSVA showing decreases in HIF, EMT, and glycolysis scores upon HBO exposure in bleomycin-challenged mice lungs (Fig. 5A–C).

The effects of HBO on the HIF activity in the lungs from mice challenged with bleomycin were verified by checking several HIF target genes, including *Adm*, *Cdkn3*, *Eno1*, *Pgam1*, *Slc2a1*, and *Tubb6*. All their expressions were

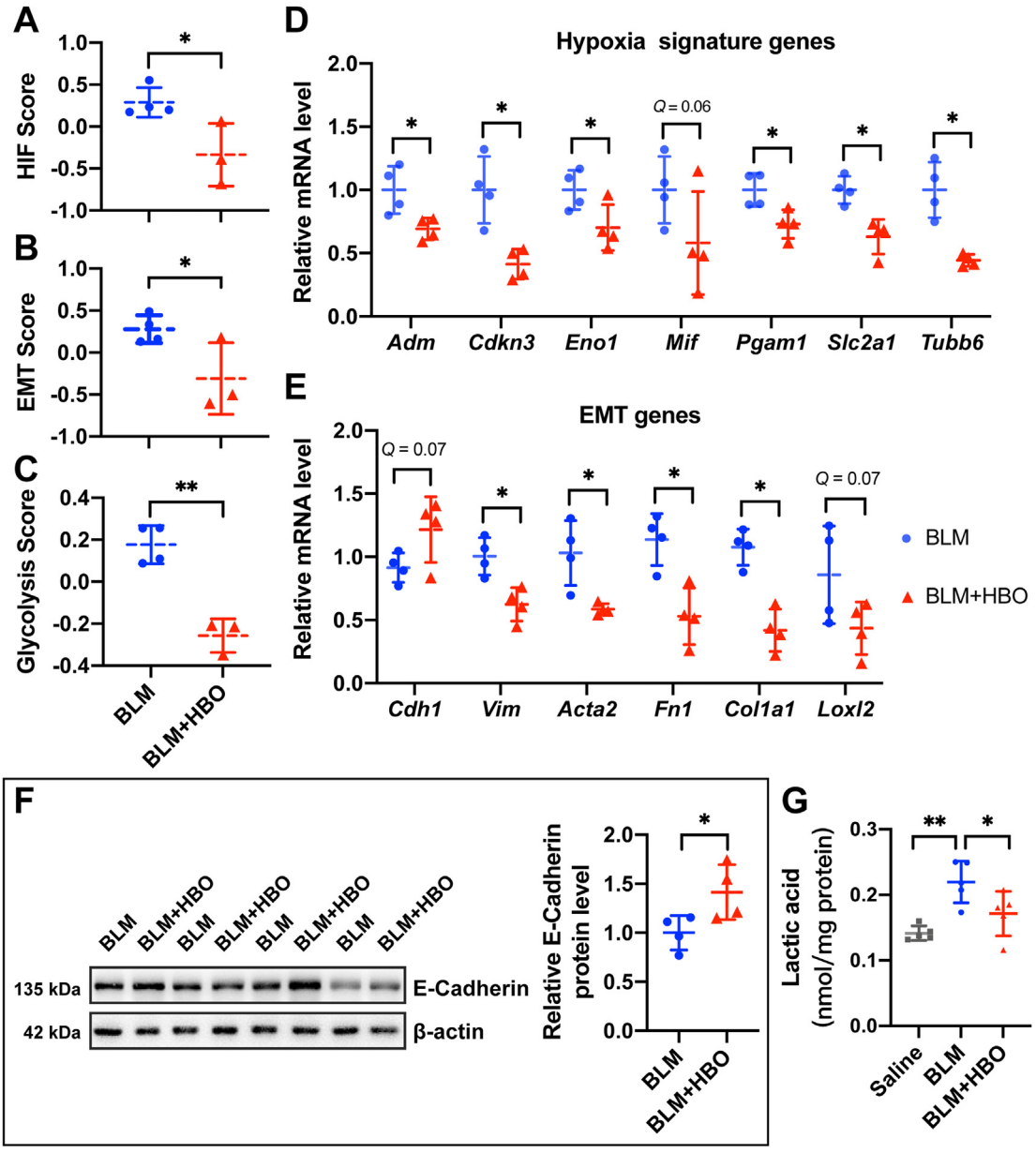

Fig. 5 Effects of hyperbaric oxygen (HBO) treatment on hypoxia, epithelial-to-mesenchymal transition and glycolysis. **(A–C)** Graphs showing the HIF score (A), EMT score (B) and glycolysis score (C) in the lungs from bleomycin-challenged mice (BLM) or bleomycin-challenged mice with repetitive HBO exposure (BLM + HBO). *$P < 0.05$, **$P < 0.01$, by two-sample *t*-test. **(D,E)** Fold change in the mRNA levels of multiple HIF target genes (D) and EMT markers (E) in the lungs from bleomycin-challenged mice (BLM) or bleomycin-challenged mice treated with repetitive HBO exposure (BLM + HBO) at 21 d post bleomycin instillation. *Actb* (β-actin)-normalized mRNA levels in the BLM group were used to set the baseline value at unity. Data are mean ± s.d. *$Q < 0.05$, **$Q < 0.01$, by two-sample Mann–Whitney *U* test, multiple comparisons using false discovery rate (*Q*) with the method of two-stage step-up (Benjamini, Krieger and Yekutieli). **(F)** Protein expression of E-cadherin in the lungs from bleomycin-challenged mice (BLM) or bleomycin-challenged mice treated with repetitive HBO exposure (BLM + HBO). β-actin was used as a loading control. β-actin-normalized protein levels in bleomycin-challenged mice lungs (BLM) were used to set the baseline value at unity. Data are mean ± s.d., $n = 4$ samples in each group. *$P < 0.05$, analyzed by two sample *t* test. **(G)** The lactate level in mice lungs with the indicated treatment. Data are mean ± s.d., $n = 5$ samples in each group. *$P < 0.05$, **$P < 0.01$, analyzed by one-way ANOVA test.

Please cite this article as: Yuan Y et al., Integrated analysis reveals the protective mechanism and therapeutic potential of hyperbaric oxygen against pulmonary fibrosis, Genes & Diseases, https://doi.org/10.1016/j.gendis.2022.08.012

decreased upon HBO exposure in bleomycin-challenged mice lungs (Fig. 5D; all Q values < 0.05, except for *Mif* with $Q = 0.06$). EMT induction in bleomycin-challenged mice lungs was also blocked by HBO exposure, at least partially, reflected by an increase in mRNA expression of *Cdh1* (E-cadherin, $Q = 0.07$), and a significant reduction in *Vim, Acta2, Fn1, and Col1a1* (Fig. 5E; all Q values < 0.05). The effect of HBO on E-cadherin was further confirmed using western blots showing that its protein level was increased upon HBO treatment in the lungs of the bleomycin-challenged mice (Fig. 5F; $P < 0.05$). In addition, we observed an elevated lactate level (a marker of glycolytic shift) in the lungs of the bleomycin-challenged mice, and this was reduced upon HBO treatment (Fig. 5G). Together these data supported the roles of HBO treatment in inhibiting EMT and glycolysis.

Discussion

In this study, several potential mechanisms of relevance to pulmonary fibrosis were identified, including increased EMT and glycolysis, which are strong independent predictors of mortality in IPF patients. These processes are potentially driven by hypoxia and blocked by HBO treatment.

The role of EMT in pulmonary fibrosis has been proposed previously.[19–21] Recent studies suggest that instead of contributing to the extracellular matrix producing fibroblast population directly, alveolar epithelial type II (ATII) cells undergoing EMT promotes a pro-fibrotic microenvironment through paracrine signalings, which enhances TGF-β-induced fibroblast activation.[22–26] Glycolytic reprogramming is found to be active in IPF patients,[27,28] and promotes myofibroblast differentiation,[29] a key event in pulmonary fibrosis formation. Glycolysis inhibition is proven to alleviate pulmonary fibrosis in bleomycin-induced mouse model.[30–32] Hypoxia is known to drive EMT and glycolytic shift,[29,33–35] and HIF is required for these processes.[29,33,34] As a hallmark feature of pulmonary fibrosis,[36,37] hypoxia signaling pathway has been found active in IPF patients,[38–46] while HIF is upregulated in lung tissues from both IPF patients and the bleomycin-induced pulmonary fibrosis mouse model.[17,39,41,44,47] Consistent with these reports, the HIF score was significantly increased in bleomycin-challenged mice lungs, IPF lungs as well as BAL samples from IPF patients, and its increase correlated with an upregulated EMT and glycolysis signature.

Since HBO increases the partial pressure of oxygen, the soluble oxygen in plasma, and the diffuse distance of oxygen,[48] it has been shown to counter tissue hypoxia with high efficacy. HBO alleviates hypoxia in multiple conditions, including the hypoxemia caused by COVID-19 infection,[49] solid tumors,[50–52] and focal cerebral ischemia model.[53] In our previous study, we provided evidence that HBO treatment reduces HIF-1α levels in lung fibroblast induced by TGF-β,[5] supports the role of HBO in reversing hypoxia. It was reported that HBO ameliorates the EMT phenomenon in keloid tissue,[54] induces mesenchymal-to-epithelial transition in a dimethyl-alpha-benzantracene mammary rat adenocarcinoma model revealed by gene expression profiling,[55] and represses EMT and Warburg effect in hypoxic non-small cell lung cancer cells.[56] Further perturbation experiments are needed to demonstrate that the HBO treatment relies on glycolysis and/or EMT to prevent lung fibrosis.

Together with these reports, our study helps to provide a unified concept for the protective mechanism of HBO against pulmonary fibrosis: HBO alleviates hypoxia during the development of pulmonary fibrosis, so inhibiting IPF-related pathological processes such as EMT and glycolysis. Given the general safety of HBO in the long-term clinical practice,[57–59] these data suggest a realistic scenario of a prospective clinical trial in IPF patients with HBO treatment.

Author contributions

Yuan Yuan: Conceptualization, methodology, investigation, project administration, writing-original draft preparation, and funding acquisition; Guoqiang Qiao: Formal analysis, investigation, methodology, validation, and writing-original draft preparation; Jiajiao Zhou: Data curation, and validation; Yilu Zhou: methodology and software; Yali Li: Methodology; Xia Li: Supervision and funding acquisition; Zhenglin Jiang: Supervision, funding acquisition, writing-reviewing, and editing; Yihua Wang: Conceptualization, methodology, supervision, funding acquisition, writing-reviewing, and editing.

Conflict of interests

The authors declare that they have no competing interests.

Funding

Yuan Yuan was supported by Natural Science Research of Jiangsu Higher Education Institutions of China (No. 19KJB320002), the Science and Technology Project of Nantong City (No. JC2020010), and a Research Startup Fund of Nantong University. Yihua Wang was supported by the UK Medical Research Council (No. MR/S025480/1) and theUK Royal Society (No. IEC＼NSFC＼191030). Zhenglin Jiang was supported by the National Natural Science Foundation of China (No. 82171869 and 81671859). Xia Li was supported by the Science and Technology Project of Nantong City (No. MS12020019 and JC2021079).

Appendix A. Supplementary data

Supplementary data to this article can be found online at https://doi.org/10.1016/j.gendis.2022.08.012.

References

1. Richeldi L, Collard HR, Jones MG. Idiopathic pulmonary fibrosis. *Lancet*. 2017;389(10082):1941—1952.
2. Mylvaganam RJ, Bailey JI, Sznajder JI, Sala MA, Northwestern Consortium CCC. Recovering from a pandemic: pulmonary fibrosis after SARS-CoV-2 infection. *Eur Respir Rev*. 2021; 30(162), 210194.

3. Zhang C, Wu Z, Li JW, et al. Discharge may not be the end of treatment: pay attention to pulmonary fibrosis caused by severe COVID-19. *J Med Virol*. 2021;93(3):1378—1386.
4. Wu X, Liu X, Zhou Y, et al. 3-month, 6-month, 9-month, and 12-month respiratory outcomes in patients following COVID-19-related hospitalisation: a prospective study. *Lancet Respir Med*. 2021;9(7):747—754.
5. Yuan Y, Li Y, Qiao G, et al. Hyperbaric oxygen ameliorates bleomycin-induced pulmonary fibrosis in mice. *Front Mol Biosci*. 2021;8, 675437.
6. Ortega M, Fraile-Martinez O, García-Montero C, et al. A general overview on the hyperbaric oxygen therapy: applications, mechanisms and translational opportunities. *Medicina*. 2021;57(9):864.
7. Hänzelmann S, Castelo R, Guinney J. GSVA: gene set variation analysis for microarray and RNA-seq data. *BMC Bioinf*. 2013;14:7.
8. Buffa FM, Harris AL, West CM, Miller CJ. Large meta-analysis of multiple cancers reveals a common, compact and highly prognostic hypoxia metagene. *Br J Cancer*. 2010;102(2):428—435.
9. Ye Y, Hu Q, Chen H, et al. Characterization of hypoxia-associated molecular features to aid hypoxia-targeted therapy. *Nat Metab*. 2019;1(4):431—444.
10. Prasse A, Binder H, Schupp JC, et al. *BAL* cell gene expression is indicative of outcome and airway basal cell involvement in idiopathic pulmonary fibrosis. *Am J Respir Crit Care Med*. 2019;199(5):622—630.
11. Liberzon A, Birger C, Thorvaldsdóttir H, Ghandi M, Mesirov JP, Tamayo P. The molecular signatures database hallmark gene set collection. *Cell Syst*. 2015;1(6):417—425.
12. Ley B, Ryerson CJ, Vittinghoff E, et al. A multidimensional index and staging system for idiopathic pulmonary fibrosis. *Ann Intern Med*. 2012;156(10):684—691.
13. Hapke RY, Haake SM. Hypoxia-induced epithelial to mesenchymal transition in cancer. *Cancer Lett*. 2020;487:10—20.
14. Tam SY, Wu VWC, Law HKW. Hypoxia-induced epithelial-mesenchymal transition in cancers: HIF-1α and beyond. *Front Oncol*. 2020;10:486.
15. Denko NC. Hypoxia, HIF1 and glucose metabolism in the solid tumour. *Nat Rev Cancer*. 2008;8(9):705—713.
16. Kierans SJ, Taylor CT. Regulation of glycolysis by the hypoxia-inducible factor (HIF):implications for cellular physiology. *J Physiol*. 2021;599(1):23—37.
17. Zhou Y, Ewing RM, Davies DE, Wang Y, Jones MG. A validated hypoxia-inducible factor (HIF) signature across tissue compartments predicts clinical outcome in human lung fibrosis. Preprint at https://www.medrxiv.org/content/10.1101/2022.01.11.22269085v1.
18. Yuan Y, Zhou Y, Li Y, et al. Deconvolution of RNA-seq analysis of hyperbaric oxygen-treated mice lungs reveals mesenchymal cell subtype changes. *Int J Mol Sci*. 2020;21(4):1371.
19. Sakuma Y. Epithelial-to-mesenchymal transition and its role in EGFR-mutant lung adenocarcinoma and idiopathic pulmonary fibrosis. *Pathol Int*. 2017;67(8):379—388.
20. Salton F, Volpe MC, Confalonieri M. Epithelial-Mesenchymal transition in the pathogenesis of idiopathic pulmonary fibrosis. *Medicina*. 2019;55(4):83.
21. Phan THG, Paliogiannis P, Nasrallah GK, et al. Emerging cellular and molecular determinants of idiopathic pulmonary fibrosis. *Cell Mol Life Sci*. 2021;78(5):2031—2057.
22. Yao L, Conforti F, Hill C, et al. Paracrine signalling during ZEB1-mediated epithelial-mesenchymal transition augments local myofibroblast differentiation in lung fibrosis. *Cell Death Differ*. 2019;26(5):943—957.
23. Hill C, Jones MG, Davies DE, Wang Y. Epithelial-mesenchymal transition contributes to pulmonary fibrosis via aberrant epithelial/fibroblastic cross-talk. *J Lung Health Dis*. 2019;3(2):31—35.
24. Yao L, Zhou Y, Li J, et al. Bidirectional epithelial-mesenchymal crosstalk provides self-sustaining profibrotic signals in pulmonary fibrosis. *J Biol Chem*. 2021;297(3), 101096.
25. Zhou Y, Hill C, Yao L, et al. Quantitative proteomic analysis in alveolar type II cells reveals the different capacities of RAS and TGF-β to induce epithelial-mesenchymal transition. *Front Mol Biosci*. 2021;8, 595712.
26. Hill C, Li J, Liu D, et al. Autophagy inhibition-mediated epithelial-mesenchymal transition augments local myofibroblast differentiation in pulmonary fibrosis. *Cell Death Dis*. 2019;10:591.
27. Maher TM. Aerobic glycolysis and the Warburg effect. an unexplored realm in the search for fibrosis therapies? *Am J Respir Crit Care Med*. 2015;192(12):1407—1409.
28. Chen Z, Liu M, Li L, Chen L. Involvement of the Warburg effect in non-tumor diseases processes. *J Cell Physiol*. 2018;233(4):2839—2849.
29. Goodwin J, Choi H, Hsieh MH, et al. Targeting hypoxia-inducible factor-1α/pyruvate dehydrogenase kinase 1 axis by dichloroacetate suppresses bleomycin-induced pulmonary fibrosis. *Am J Respir Cell Mol Biol*. 2018;58(2):216—231.
30. Xie N, Tan Z, Banerjee S, et al. Glycolytic reprogramming in myofibroblast differentiation and lung fibrosis. *Am J Respir Crit Care Med*. 2015;192(12):1462—1474.
31. Chen W, Zhang J, Zhong W, et al. Anlotinib inhibits PFKFB3-driven glycolysis in myofibroblasts to reverse pulmonary fibrosis. *Front Pharmacol*. 2021;12, 744826.
32. Wang Z, Chen L, Huang Y, et al. Pharmaceutical targeting of succinate dehydrogenase in fibroblasts controls bleomycin-induced lung fibrosis. *Redox Biol*. 2021;46, 102082.
33. Delbrel E, Uzunhan Y, Soumare A, et al. ER stress is involved in epithelial-to-mesenchymal transition of alveolar epithelial cells exposed to a hypoxic microenvironment. *Int J Mol Sci*. 2019;20(6):1299.
34. Zhou G, Dada LA, Wu M, et al. Hypoxia-induced alveolar epithelial-mesenchymal transition requires mitochondrial ROS and hypoxia-inducible factor 1. *Am J Physiol Lung Cell Mol Physiol*. 2009;297(6):L1120—L1130.
35. Guo L, Xu JM, Liu L, Liu SM, Zhu R. Hypoxia-induced epithelial-mesenchymal transition is involved in bleomycin-induced lung fibrosis. *BioMed Res Int*. 2015;2015, 232791.
36. Lokmic Z, Musyoka J, Hewitson TD, Darby IA. Hypoxia and hypoxia signaling in tissue repair and fibrosis. *Int Rev Cell Mol Biol*. 2012;296:139—185.
37. Plantier L, Cazes A, Dinh-Xuan AT, Bancal C, Marchand-Adam S, Crestani B. Physiology of the lung in idiopathic pulmonary fibrosis. *Eur Respir Rev*. 2018;27(147), 170062.
38. Yamazaki R, Kasuya Y, Fujita T, et al. Antifibrotic effects of cyclosporine A on TGF-β1-treated lung fibroblasts and lungs from bleomycin-treated mice: role of hypoxia-inducible factor-1α. *Faseb J*. 2017;31(8):3359—3371.
39. Tzouvelekis A, Harokopos V, Paparountas T, et al. Comparative expression profiling in pulmonary fibrosis suggests a role of hypoxia-inducible factor-1 alpha in disease pathogenesis. *Am J Respir Crit Care Med*. 2007;176(11):1108—1119.
40. Qian F, He M, Duan W, et al. Cross regulation between hypoxia-inducible transcription factor-1α (HIF-1α) and transforming growth factor (TGF)-ß1 mediates nickel oxide nanoparticles (NiONPs)-induced pulmonary fibrosis. *Am J Transl Res*. 2015;7(11):2364—2378.
41. Aquino-Gálvez A, González-Ávila G, Jiménez-Sánchez LL, et al. Dysregulated expression of hypoxia-inducible factors augments myofibroblasts differentiation in idiopathic pulmonary fibrosis. *Respir Res*. 2019;20(1):130.

Please cite this article as: Yuan Y et al., Integrated analysis reveals the protective mechanism and therapeutic potential of hyperbaric oxygen against pulmonary fibrosis, Genes & Diseases, https://doi.org/10.1016/j.gendis.2022.08.012

42. Xie H, Tan JT, Wang RL, Meng XX, Tang X, Gao S. Expression and significance of HIF-1α in pulmonary fibrosis induced by paraquat. *Exp Biol Med*. 2013;238(9):1062—1068.
43. Philip K, Mills TW, Davies J, et al. HIF1A up-regulates the ADORA2B receptor on alternatively activated macrophages and contributes to pulmonary fibrosis. *Faseb J*. 2017;31(11): 4745—4758.
44. Ueno M, Maeno T, Nomura M, et al. Hypoxia-inducible factor-1α mediates TGF-β-induced PAI-1 production in alveolar macrophages in pulmonary fibrosis. *Am J Physiol Lung Cell Mol Physiol*. 2011;300(5):L740—L752.
45. Kusko RL, Brothers 2nd JF, Tedrow J, et al. Integrated genomics reveals convergent transcriptomic networks underlying chronic obstructive pulmonary disease and idiopathic pulmonary fibrosis. *Am J Respir Crit Care Med*. 2016;194(8):948—960.
46. Burman A, Kropski JA, Calvi CL, et al. Localized hypoxia links ER stress to lung fibrosis through induction of C/EBP homologous protein. *JCI Insight*. 2018;3(16), e99543.
47. Brereton CJ, Yao L, Davies ER, et al. Pseudohypoxic HIF pathway activation dysregulates collagen structure-function in human lung fibrosis. *Elife*. 2022;11, e69348.
48. Choudhury R. Hypoxia and hyperbaric oxygen therapy: a review. *Int J Gen Med*. 2018;11:431—442.
49. Paganini M, Bosco G, Perozzo FAG, et al. The role of hyperbaric oxygen treatment for COVID-19:a review. *Adv Exp Med Biol*. 2021;1289:27—35.
50. Kinoshita Y, Kohshi K, Kunugita N, Tosaki T, Yokota A. Preservation of tumour oxygen after hyperbaric oxygenation monitored by magnetic resonance imaging. *Br J Cancer*. 2000;82(1):88—92.
51. Beppu T, Kamada K, Yoshida Y, Arai H, Ogasawara K, Ogawa A. Change of oxygen pressure in glioblastoma tissue under various conditions. *J Neuro Oncol*. 2002;58(1):47—52.
52. Thews O, Vaupel P. Temporal changes in tumor oxygenation and perfusion upon normo- and hyperbaric inspiratory hyperoxia. *Strahlenther Onkol*. 2016;192(3):174—181.
53. Sun L, Marti HH, Veltkamp R. Hyperbaric oxygen reduces tissue hypoxia and hypoxia-inducible factor-1 alpha expression in focal cerebral ischemia. *Stroke*. 2008;39(3):1000—1006.
54. Zhang M, Liu S, Guan E, et al. Hyperbaric oxygen therapy can ameliorate the EMT phenomenon in keloid tissue. *Medicine*. 2018;97(29), e11529.
55. Moen I, Øyan AM, Kalland KH, et al. Hyperoxic treatment induces mesenchymal-to-epithelial transition in a rat adenocarcinoma model. *PLoS One*. 2009;4(7), e6381.
56. Zhang L, Ke J, Min S, et al. Hyperbaric oxygen therapy represses the Warburg effect and epithelial-mesenchymal transition in hypoxic NSCLC cells *via* the HIF-1α/PFKP axis. *Front Oncol*. 2021;11, 691762.
57. Camporesi EM. Side effects of hyperbaric oxygen therapy. *Undersea Hyperb Med*. 2014;41(3):253—257.
58. Hadanny A, Meir O, Bechor Y, Fishlev G, Bergan J, Efrati S. The safety of hyperbaric oxygen treatment: retrospective analysis in 2, 334 patients. *Undersea Hyperb Med*. 2016; 43(2):113—122.
59. Hadanny A, Zubari T, Tamir-Adler L, et al. Hyperbaric oxygen therapy effects on pulmonary functions: a prospective cohort study. *BMC Pulm Med*. 2019;19(1):148.

Please cite this article as: Yuan Y et al., Integrated analysis reveals the protective mechanism and therapeutic potential of hyperbaric oxygen against pulmonary fibrosis, Genes & Diseases, https://doi.org/10.1016/j.gendis.2022.08.012